International Journal of Control

ISSN: (Print) (Online) Journal homepage: www.tandfonline.com/journals/tcon20

Spectral-based optimal output-feedback boundary control of a cracking catalytic reactor PDE model

Ilyasse Aksikas

To cite this article: Ilyasse Aksikas (12 Jan 2024): Spectral-based optimal output-feedback boundary control of a cracking catalytic reactor PDE model, International Journal of Control, DOI: 10.1080/00207179.2024.2302057

To link to this article: https://doi.org/10.1080/00207179.2024.2302057

Published online: 12 Jan 2024.

Submit your article to this journal

Article views: 33

View related articles

View Crossmark data

Full Terms & Conditions of access and use can be found at
https://www.tandfonline.com/action/journalInformation?journalCode=tcon20

INTERNATIONAL JOURNAL OF CONTROL
https://doi.org/10.1080/00207179.2024.2302057

Taylor & Francis
Taylor & Francis Group

Check for updates

Spectral-based optimal output-feedback boundary control of a cracking catalytic reactor PDE model

Ilyasse Aksikas

Department of Mathematics, Statistics and Physics, College of Arts and Science, Qatar University, Doha, Qatar

ABSTRACT
This research paper focuses on the design of a boundary optimal controller with output feedback for a tubular catalytic cracking reactor. The process is represented by a set of non-linear parabolic partial differential equations (PDEs). The approach involves utilising the linearised infinite-dimensional version of the model, taking advantage of the system generator being a Riesz spectral operator. A stabilising compensator is designed by leveraging the eigenvalues and eigenvectors of the system generator. This paper also includes numerical simulations to demonstrate the performance of the developed algorithm.

ARTICLE HISTORY
Received 4 May 2023
Accepted 30 December 2023

KEYWORDS
Catalytic cracking process; output feedback control; boundary control; optimal control; parabolic PDEs; Riesz spectral operator

1. Introduction

Many chemical and biochemical reactor processes can be modelled by parabolic partial differential equations (PDEs). Indeed, these types of models capture the diffusion, convection and reaction, which are the main features in the dynamics of a chemical process (see Aksikas et al., 2004; Christofides, 1998, 2001; Ray, 1981). In general, the control and estimation of PDEs have attracted lots of attention and it represent a huge area of research (Ahmed-Ali et al., 2015; Christofides & Daoutidis, 1996; Liu et al., 2019; Shang et al., 2000; Sira-Ramirez, 1989; Smyshlyaev & Krstic, 2005 to cite a few). Besides that, the control of chemical reactors is a significant and fertile domain for research. A large portion of these research works was dedicated to control developments based on ordinary differential equation (ODE) models (see Ray, 1981 and references therein). On the other hand, PDE model-based control of chemical tubular reactors has garnered considerable interest and focus and usually divided into two major approaches. The first one is based on discretisation techniques in which the PDE model is transformed to an ODE model and the latter is employed for control system design. In Li and Christofides (2008), optimal control for transport–reaction processes has been solved by using two different discretisation methods to create reduced-order models appropriate for control design. On the other hand, model predictive control has been developed for parabolic PDE model in Dubljevic et al. (2006) and Dubljevic and Christofides (2006) by using modal decomposition approach and furthermore the case study of a tubular reactor with recycle has been explored in Khatibi et al. (2021). The design was based on the discrete version of the PDE model by using Cayley–Tustin scheme. In Bošković and Krstić (2002), backstepping design has been used to control tubular reactors. The main objective is to achieve the stabilisation of an unstable equilibrium profile by implementing boundary control at the inlet of the tubular reactor. The original nonlinear PDE model has been discretised by using finite-difference approximation and a global stabilising boundary feedback control is developed. The method of characteristics is also a very important technique that is widely used to control chemical processes modelled by hyperbolic PDEs (see, e.g. Hanczyz & Palazoglu, 1995; Pakravesh et al., 2016). It is not a discretisation method but it allows to convert PDE model into ODEs along the characteristics curves.

The second approach is based on infinite-dimensional state–space representation on which control techniques are implemented. Linear-quadratic control has been solved for different types of chemical processes by using infinite-dimensional abstract representation (see, e.g. Aksikas et al., 2013; Moghadam et al., 2012; Mohammadi et al., 2012). In Bošković et al. (2003), backstepping control in infinite-dimensional setting is solved for a class of parabolic distributed parameter systems with application to an unstable tubular chemical reactor. Indeed, stabilisation is attained by establishing coordinate transformations in the form of recursive relationships. Another technique to stabilise tubular reactor is to use Lyapunov-based control (Zhou et al., 2015). Stabilisation is accomplished through the utilisation of a Lyapunov function obtained from the second law of thermodynamics, known as the availability function. Finally, output feedback regulation and observer designs were the objective of many research works (see, e.g. Bounit & Hammouri, 1997; Christofides & Daoutidis, 1996; Liu et al., 2022; Vries et al., 2007; Xu et al., 1995). In Reyes et al. (2020), a nonlinear passive output feedback regulator has been designed to stabilise an unstable tubular reactor. Recently, duality feature has been used to design observers for tubular reactors (see, e.g. Aksikas, 2020, 2021a, 2021b). This feature has been used before in Deutscher (2013) to design a finite-dimensional state-feedback control for a boundary control linear system.

CONTACT Ilyasse Aksikas aksikas@qu.edu.qa

© 2024 Informa UK Limited, trading as Taylor & Francis Group

A very important chemical process is the catalytic cracking reactor (CCR). Primarily employed within petroleum refineries, catalytic cracking serves the purpose of transforming hydrocarbon fractions extracted from crude oils into gasoline, olefinic gases and various other products. The principal impetus for enhancing the catalytic cracking process stems from the need to produce increased quantities of gases while witnessing a reduced demand for residual oils. Moreover, it has more advantages than the thermal cracking method. Indeed, it maximises the gasoline production with higher octane rating and also it has more economic value (see Gary & Handwerk, 2001). In Mohammadi et al. (2012), a state-feedback optimal controller is designed with the objective to drive the CCR process towards its desired steady state. However, this approach assumes that full information about the system states is available, which is not a practical scenario. In this paper, the boundary output-feedback control problem will be solved for the CCR system based on the associated PDE model. This involves the design of an observer to estimate the system states. The main challenge here is the fact that the catalytic cracking process is a boundary control system, which means that an augmented version of the system on an extended state space is to be used for the purpose of the control design. Moreover, the system generator is a Riesz spectral operator, namely, a linear closed operator with simple eigenvalues and the corresponding eigenvectors form a Riesz basis (see Curtain & Zwart, 1995). One of the main advantages is the fact that a Riesz spectral operator as well as its resolvent can be expressed as an infinite series in terms of the associated eigenvectors. Moreover, the spectral approach enables the selection of the number of nodes to achieve desired regulator performance and/or convergence speed. Here, the primary purpose of this paper is to explore how the spectral approach can be implemented to design an optimal boundary output-feedback regulator for the crucial process of cracking reactor. This introduction section is concluded by highlighting the main contributions of this work:

(1) Spectral and dynamical properties of the cracking reactor PDE model have been studied and analysed in great details.
(2) Optimal output-feedback boundary control has been designed and formulated as a series expansion of the eigenvectors of the system generator.
(3) A stabilising compensator has been formulated by using the spectral approach in which the components are generated by a set of differential equations.
(4) Numerical simulations are performed to test the designed output regulator.

Notations: Let $L^2(0,1)$ be the space of measurable square integrable real-valued functions on $[0,1]$ equipped with the inner product and norm for all $f_1, g_1 \in L^2(0,1)$

$$\langle f_1, g_1\rangle_2 = \int_0^1 f_1(\xi) g_1(\xi)\,\mathrm{d}\xi \quad \text{and} \quad \|f_1\|_2 = \sqrt{\langle f_1, f_1\rangle_2}$$

Denote by $H = L^2(0,1) \oplus L^2(0,1)$ (the cartesian product of $L^2(0,1)$ and itself) the Hilbert space equipped with the usual inner product and norm for all $f = (f_1, f_2)^T, g = (g_1, g_2)^T \in H$

$$\langle f, g\rangle_H = \langle f_1, g_1\rangle_2 + \langle f_2, g_2\rangle_2 \quad \text{and} \quad \|f\|_H = \sqrt{\|f_1\|_2^2 + \|f_2\|_2^2}$$

Denote by $\mathcal{H} = \mathbb{R} \oplus H$ the space obtained as the cartesian product of the space H and $\mathbb{R}$. $\mathcal{H}$ is equipped by the inner product and norm for all $\bar{f} = (w_1, f)^T, \bar{g} = (w_2, g)^T \in \mathcal{H}$.

$$\langle \bar{f}, \bar{g}\rangle = w_1 w_2 + \langle f, g\rangle_H \quad \text{and} \quad \|\bar{f}\| = \sqrt{w_1^2 + \|f\|_H^2}$$

On the other hand, $L^\infty(0,1)$ is the space of bounded measurable functions on $[0,1]$. ■

2. Mathematical model

The transport–reaction process investigated in this paper is a tubular catalytic cracking reactor This chemical process involves the following reactions:

$$A \overset{k_1}{\to} B \overset{k_2}{\to} C \quad \text{and} \quad A \overset{k_3}{\to} C,$$

where A is the gas oil, B is the gasoline and C represents other products such as butanes, coke and so on. If we assume that the process is isothermal, then the dynamics of the plant can be modelled by the following parabolic PDEs (see Weekman, 1969).

$$\begin{cases} \dfrac{\partial Y_1}{\partial t} = D_a \dfrac{\partial^2 Y_1}{\partial \xi^2} - v\dfrac{\partial Y_1}{\partial \xi} - k_0 Y_1^2 \\ \dfrac{\partial Y_2}{\partial t} = D_a \dfrac{\partial^2 Y_2}{\partial \xi^2} - v\dfrac{\partial Y_2}{\partial \xi} + k_1 Y_1^2 - k_2 Y_2. \end{cases} \tag{1}$$

Note that the reaction rate equations are based on experimental data done in Weekman (1969). The boundary and initial conditions are

$$\begin{aligned} &D_a \frac{\partial Y_1}{\partial \xi}(t,0) = v(Y_1(t,0) - Y_{1,in}) \\ &D_a \frac{\partial Y_2}{\partial \xi}(t,0) = v(Y_2(t,0) - Y_{2,in}) \\ &\frac{\partial Y_1}{\partial \xi}(t,L) = \frac{\partial Y_2}{\partial \xi}(t,L) = 0 \\ &Y_1(0,\xi) = f_1(\xi) \quad \text{and} \quad Y_2(0,\xi) = f_2(\xi). \end{aligned} \tag{2}$$

Y_1 and Y_2 are the weight fractions of components A and B, respectively. t and ξ represent the time and space variables. D_a and v are the axial dispersion coefficient and the superficial velocity. $k_0 := k_1 + k_3$, where $k_i, 1 \le i \le 3$ are the stoichiometric coefficients of the reactions described above. $Y_{1,in}$ and $Y_{2,in}$ are the inlet weight fractions of components A and B, respectively. Note that $Y_{2,in}$ is assumed to be constant.

Usually, convection–diffusion–reaction non-isothermal process with Arrhenius-type reaction rate model generates multiple equilibrium points, either stable or unstable (Dochain, 2016; Varma & Amundson, 1973). On the other hand, this kind of process can be seen as intermediate model between the plug flow reactor (i.e. negligible diffusion) and CSTR model. It is known that the plug flow reactor admits only one steady state while the CSTR can exhibit three different equilibrium points, which means that multiplicity (or uniqueness) of steady-states depends on the diffusion coefficient. In this paper, the process is isothermal and the reaction rate is proportional to the square of reactant Y_1. The corresponding equilibrium equations are given by the following second-order differential equations:

$$\begin{cases} D_a \dfrac{d^2\overline{Y}_1}{d\xi^2} - v\dfrac{d\overline{Y}_1}{d\xi} - k_0\overline{Y}_1^2 = 0 \\ D_a \dfrac{d^2\overline{Y}_2}{d\xi^2} - v\dfrac{d\overline{Y}_2}{d\xi} + k_1\overline{Y}_1^2 - k_2\overline{Y}_2 = 0. \end{cases} \tag{3}$$

Similarly to the study done in Dochain (2016), the multiplicity of steady states can be investigated but this is out of the framework of this paper. Here, let us consider a general steady state for the process denoted by $\overline{Y}_1$ and $\overline{Y}_2$ under the control input $\overline{Y}_{1,in}$. Note that $\overline{Y}_1$ and $\overline{Y}_2$ can be obtained by numerically solving Equation (3). The main objective in this section is to write the linearised infinite-dimensional version of the PDE model around the steady state. To convert the non-linear diffusion–convection–reaction system into a linear diffusion–reaction system, the following weighted state deviation is implemented.

$$z(t) = \begin{bmatrix} z_1(t) \\ z_2(t) \end{bmatrix} = e^{-\frac{v\xi}{2D_a}} \begin{bmatrix} Y_1(t) - \overline{Y}_1 \\ Y_2(t) - \overline{Y}_2 \end{bmatrix} \quad \text{and}$$
$$w(t) = v(Y_{1,in} - \overline{Y}_{1,in}). \tag{4}$$

By straightforward calculations, these transformations will lead to the following boundary control linear infinite-dimensional system on the Hilbert space H:

$$\begin{cases} \dot{z}(t) = \mathcal{A}z(t), \quad z(0) = z_0 \\ \mathcal{B}z(t) = w(t) \\ y(t) = \mathcal{C}z(t) \end{cases} \tag{5}$$

where the operator $\mathcal{A}$ is defined on

$$D(\mathcal{A}) = \Big\{ z \in H : z, \frac{dz}{d\xi} \text{ are absolutely continuous,} \\ \frac{d^2 z}{d\xi^2} \in H, D_a\frac{\partial z_i(0,t)}{\partial \xi} + \frac{v}{2}z_i(0,t) = 0, \\ (i = 1, 2) \text{ and } D_a\frac{\partial z_2(1,t)}{\partial \xi} - \frac{v}{2}z_2(1,t) = 0 \Big\}$$

$$\text{by} \quad \mathcal{A} = \begin{pmatrix} D_a\dfrac{d^2}{d\xi^2} + m_{11}(\xi) & 0 \\ m_{21}(\xi) & D_a\dfrac{d^2}{d\xi^2} + m_{22} \end{pmatrix} \\ := \begin{pmatrix} \mathcal{A}_{11} & 0 \\ \mathcal{A}_{21} & \mathcal{A}_{22} \end{pmatrix} \tag{6}$$

such that the functions m_{ij} are given by $m_{11}(\xi) = -\frac{v}{4D_a} - 2k_0\overline{Y}_1(\xi)$, $m_{21}(\xi) = 2k_1\overline{Y}_1(\xi)$ and $m_{22} = -\frac{v}{4D_a} - k_2$. The input operator $\mathcal{B} : H \to \mathbb{R}$ is

$$z = \begin{pmatrix} z_1 \\ z_2 \end{pmatrix} \mapsto \mathcal{B}z = \left(-D_a\frac{d}{d\xi} + \frac{v}{2} 0\right)\begin{pmatrix} z_1 \\ z_2 \end{pmatrix}_{|\xi=0} \tag{7}$$

and the output function is given by $y(t) = \mathcal{C}z(t)$, where $\mathcal{C} : H \to \mathbb{R}$ is given by

$$z = \begin{pmatrix} z_1 \\ z_2 \end{pmatrix} \mapsto \mathcal{C}z = \int_0^1 (c_1z_1 + c_2z_2)\, d\xi = \langle \mathbf{c}, z\rangle_H, \tag{8}$$

where $\mathbf{c} = [c_1 \quad c_2]^T$, c_1 and c_2 are space-dependent functions in $L^\infty(0, 1)$ that can be weight functions or also they can be used to specify sensor locations.

At this stage, it is very important to convert the boundary control system (5) into the standard form of a general infinite-dimensional linear dynamical system. To do so, the process given in Curtain and Zwart (1995, section 3.3, p. 121) is adopted here. Indeed, the process consists of two main steps. The first step is devoted to find a bounded operator $B \in \mathcal{L}(\mathbb{R}, H)$ such that the following conditions hold: (i) for all $w \in \mathbb{R}$, $Bw \in D(\mathcal{A})$, (ii) the operator $\mathcal{A}B$ is a bounded operator and (iii) $\forall\, w \in \mathbb{R}$, $\mathcal{B}Bw = w$. With this aim in mind, let us define the operator $B : \mathbb{R} \to H$ by

$$Bw = \mathbf{b}(\xi)w \in H, \tag{9}$$

where $\mathbf{b}$ is a continuous vector function on $[0, 1]$. It is obvious to observe that if the vector function $\mathbf{b}$ fulfils the following criteria:

$$D_a\frac{d\mathbf{b}}{d\xi}(0) = \frac{v}{2}\mathbf{b}(0) - \begin{bmatrix} 1 \\ 0 \end{bmatrix} \quad \text{and} \quad D_a\frac{d\mathbf{b}}{d\xi}(1) = -\frac{v}{2}\mathbf{b}(1), \tag{10}$$

then the operator B satisfies the conditions (i), (ii) and (iii) given above. To have more degrees of freedom, it is decided to keep $\mathbf{b}$ as an unknown vector.

The second step of the approach is dedicated to write the boundary control system under the standard form. Let us introduce the new state and the new input as follows:

$$x(t) := \begin{bmatrix} w(t) \\ \tilde{z}(t) \end{bmatrix} := \begin{bmatrix} w(t) \\ z(t) - Bw(t) \end{bmatrix} \\ \in \mathcal{H} := \mathbb{R} \oplus H \quad \text{and} \quad u(t) = \dot{w}(t) \tag{11}$$

and the new operator $A : D(A) \to H$, which has the same expression as the operator $\mathcal{A}$ but its domain is slightly modified and becomes

$$D(A) = D(\mathcal{A}) \cap Ker(\mathcal{B}) \\ = \Big\{ \mathbf{h} \in H : \mathbf{h}, \frac{d\mathbf{h}}{d\xi} \text{ absolutely continuous,} \\ \frac{d^2\mathbf{h}}{d\xi^2} \in H,\ D_a\frac{d\mathbf{h}(0)}{d\xi} - \frac{v}{2}\mathbf{h}(0) = 0, \\ D_a\frac{\mathbf{h}(1)}{d\xi} + \frac{v}{2}\mathbf{h}(1) = 0 \Big\}.$$

Then the differentiation of the new state will lead to the following linear augmented system on the new state space $\mathcal{H}$:

$$\begin{cases} \dot{x}(t) = \hat{A}x(t) + \hat{B}u(t) \quad x(0) = x_0 \\ y(t) = \hat{C}x(t), \end{cases} \tag{12}$$

where the new operators $\hat{A}, \hat{B}$ and $\hat{C}$ are given by

$$\hat{A} = \begin{bmatrix} 0 & 0 \\ \mathcal{A}B & \mathcal{A} \end{bmatrix}; \quad \hat{B} = \begin{bmatrix} I \\ -B \end{bmatrix}, \quad \hat{C} = [\mathcal{C}B \quad \mathcal{C}]. \tag{13}$$

The operator $\mathcal{A}B$ can be expressed by taking into consideration the fact that it acts on elements of $\mathbb{R}$.

$$\mathcal{A}B = \left(D_a \frac{d^2\mathbf{b}}{d\xi^2} + M(\xi)\mathbf{b} \right) \cdot I$$
$$:= \gamma \cdot I \quad \text{where} \quad M = \begin{pmatrix} m_{11} & 0 \\ m_{21} & m_{22} \end{pmatrix}. \tag{14}$$

Note that the adjoint operators of B and $\mathcal{C}$ are given by $B^*z = \langle \mathbf{b}, z\rangle_H \ \forall\, z \in H$ and $\mathcal{C}^*y = \mathbf{c}y, \forall y \in \mathbb{R}$, which means that the adjoint operators of $\hat{B}$ and $\hat{C}$ are given by

$$\hat{B}^* \begin{bmatrix} w \\ z \end{bmatrix} = [I \quad -B^*] \begin{bmatrix} w \\ z \end{bmatrix} = w - \langle \mathbf{b}, z\rangle_H,$$
$$\forall\, w \in \mathbb{R}, \quad \forall\, z \in H$$

and

$$\hat{C}^* y = \begin{bmatrix} B^*C^* \\ C^* \end{bmatrix} y = \begin{bmatrix} \langle \mathbf{b}, \mathbf{c}\rangle_H y \\ \mathbf{c}y \end{bmatrix}, \quad \forall\, y \in \mathbb{R}.$$

3. Dynamical properties

The objective of this section is twofold. First, the emphasis lies on the dynamical characteristics of both the boundary control system (5) and the augmented system (12). Second, the objective is to compute the eigenvalues and eigenvectors of the operators $\mathcal{A}11$, $\mathcal{A}22$, $\mathcal{A}$ and $\hat{A}$. Let us start by studying the operators $\mathcal{A}_{11}$ and $\mathcal{A}_{22}$. First it should be noted that due to the linearisation process, m_{11} is a function of the steady-state $\overline{Y}_1$ and therefore it is a space-varying function, which means that an analytical method cannot be used to calculate the eigenvalues and eigenfunctions of $\mathcal{A}_{11}$. To deal with this issue, two options can be implemented: (i) use a numerical method such as the one described in De Monte (2002) or (ii) assume that the variations of $\overline{Y}_1$ are negligible and then use its average value on the interval $[0, 1]$. In what follows, this option will be implemented for the sake of simplicity. This is not needed for the operator $\mathcal{A}_{22}$ since m_{22} is indeed constant.

Lemma 3.1: *The operators $\mathcal{A}_{11}$ and $\mathcal{A}_{22}$, given in Equation (6), are Riesz spectral operators. Moreover, they are the generators of exponentially stable C_0-semigroups on $L^2(0, 1)$.*

Proof: It is known that the operator $\mathcal{A}_{11}$ is a Sturm–Liouville operator. Also, by using Curtain and Zwart (1995, exercice 2.10, pp. 82–83), the operator $\mathcal{A}_{11}$ is closed. Moreover, the spectrum of $\mathcal{A}_{11}$ is limited to only point spectrum set. By solving the eigenvalue problem associated with $\mathcal{A}_{11}$, it can be shown that the eigenvalues are

$$\mu_n = m_{11} - D_a\omega_n^2 < 0, \quad n \geq 1, \tag{15}$$

where the sequence $\{\omega_n\}_{n\geq 1}$ is the set of solutions of the following algebraic equation:

$$\tan(\omega) = \frac{4D_a\omega\nu}{4D_a^2\omega^2 - \nu^2} \tag{16}$$

and the corresponding eigenfunctions given by

$$\phi_n = c_n \left[\cos(\omega_n z) + \frac{\nu}{2D_a\omega_n} \sin(\omega_n z) \right], \tag{17}$$

which is a Riesz basis of $L^2(0, 1)$. Moreover, the operator $\mathcal{A}_{11}$ generates an exponentially stable C_0-semigroup on $L^2(0, 1)$. Indeed, this is due to the fact that all eigenvalues are negative. Moreover, there exists $M > 0$ such that

$$\|e^{\mathcal{A}_{11}t}\|_{\mathcal{L}(L^2(0,1))} < M\, e^{\mu_n t}, \quad \forall\, t \geq 0.$$

Note that the constants $\{c_n\}_{n\geq 1}$ can be chosen such that $\{\phi_n\}_{n\geq 1}$ is an orthonormal basis of $L^2(0, 1)$, i.e. $\langle \phi_n, \phi_m\rangle_2 = \delta_{nm}$. ■

On the other hand, the operator $\mathcal{A}_{22}$ has the same form of $\mathcal{A}_{11}$ and then it has the same properties. Moreover, the eigenvalues of $\mathcal{A}_{22}$ are given as

$$\eta_n = m_{22} - D_a\omega_n^2 < 0, \quad n \geq 1 \tag{18}$$

with the associated eigenfunctions ϕ_n, given by (17).

By using the dynamical and spectral properties of $\mathcal{A}_{11}$ and $\mathcal{A}_{22}$, one can state the properties of the operators $\mathcal{A}$ and $\hat{A}$ and also calculate their eigenvalues and eigenvectors. The theorem below focuses on the characteristics of the operator $\mathcal{A}$.

Theorem 3.2: *The operator $\mathcal{A}$, as defined in Equation (6), is a Riesz spectral operator and serves as the generator of an exponentially stable C_0-semigroup on H.*

Proof: The operator $\mathcal{A}$ is a lower triangular operator with diagonal entries ($\mathcal{A}_{11}$ and $\mathcal{A}_{22}$) whose are the generators of exponentially stable C_0-semigroups on $L^2(0, 1)$. Hence, by using Curtain and Zwart (1995, lemma 3.3.2, p. 114), the operator $\mathcal{A}$ generates an exponentially stable C_0-semigroup on H. Also, the spectrum of the operator $\mathcal{A}$ is made up of the eigenvalues of the operators $\mathcal{A}_{11}$ and $\mathcal{A}_{22}$ together, i.e. $\sigma(\mathcal{A}) = \sigma(\mathcal{A}_{11} \cap \sigma(\mathcal{A}_{22})$, which are given by

$$\lambda_{2n-1} = \mu_n, \quad \text{for} \quad n \geq 1$$
$$\lambda_{2n} = \eta_n, \quad \text{for} \quad n \geq 1$$

associated with the following eigenvectors given for all $n \geq 1$ by

$$\tilde{\boldsymbol{\phi}}_{2n-1} = \begin{pmatrix} \phi_n \\ (\mu_n I - \mathcal{A}_{22})^{-1}\mathcal{A}_{21}\phi_n \end{pmatrix}$$
$$= \begin{pmatrix} \phi_n \\ \displaystyle\sum_{k=1}^{\infty} \frac{1}{\mu_n - \eta_k} \langle \mathcal{A}_{21}\phi_n, \phi_k\rangle_2 \phi_k \end{pmatrix},$$

$$\tilde{\boldsymbol{\phi}}_{2n} = \begin{pmatrix} 0 \\ \phi_n \end{pmatrix}.$$

In a similar way, one can get the spectrum of the adjoint operator $\mathcal{A}^*$, as follows:

$$\tilde{\boldsymbol{\psi}}_{2n-1} = \begin{pmatrix} \phi_n \\ 0 \end{pmatrix} \quad \text{and}$$

$$\tilde{\boldsymbol{\psi}}_{2n} = \begin{pmatrix} \displaystyle\sum_{k=1}^{\infty} \frac{1}{\eta_n - \mu_k} \langle \mathcal{A}_{21}\phi_n, \phi_k\rangle_2 \phi_k \\ \phi_n \end{pmatrix}.$$

Note that $\{\tilde{\boldsymbol{\phi}}_n\}_{n\geq 1}$ and $\{\tilde{\boldsymbol{\psi}}_n\}_{n\geq 1}$ are biorthogonal, i.e. $\langle \tilde{\boldsymbol{\phi}}_n, \tilde{\boldsymbol{\psi}}_m\rangle_H = \delta_{nm}$. Indeed, the following identities are straightforward:

$$\langle \tilde{\boldsymbol{\phi}}_{2n-1}, \tilde{\boldsymbol{\psi}}_{2m-1}\rangle_H = \langle \tilde{\boldsymbol{\phi}}_{2n}, \tilde{\boldsymbol{\psi}}_{2m}\rangle_H = \delta_{nm} \quad \text{and} \quad \langle \tilde{\boldsymbol{\phi}}_{2n}, \tilde{\boldsymbol{\psi}}_{2m-1}\rangle_H = 0.$$

Moreover, by using the expression of $\tilde{\boldsymbol{\phi}}_{2n-1}$ and $\tilde{\boldsymbol{\psi}}_{2m}$ and the inner product in H, one gets the following identity:

$$\begin{aligned}\langle \tilde{\boldsymbol{\phi}}_{2n-1}, \tilde{\boldsymbol{\psi}}_{2m}\rangle_H &= \sum_{k=1}^{\infty} \frac{1}{\eta_m - \mu_k} \langle \mathcal{A}_{21}\phi_m, \phi_k\rangle_2 \langle \phi_n, \phi_k\rangle_2 \\ &\quad + \sum_{k=1}^{\infty} \frac{1}{\mu_n - \eta_k} \langle \mathcal{A}_{21}\phi_n, \phi_k\rangle_2 \langle \phi_k, \phi_m\rangle_2 \\ &= \frac{1}{\eta_m - \mu_n} \langle \mathcal{A}_{21}\phi_m, \phi_n\rangle_2 \\ &\quad + \frac{1}{\mu_n - \eta_m} \langle \mathcal{A}_{21}\phi_k, \phi_m\rangle_2 = 0 \quad \text{since} \quad \mathcal{A}_{21} = \mathcal{A}_{21}^*.\end{aligned}$$

Now the dynamical properties of the augmented system can be stated and the eigenvalues and eigenvectors of $\hat{A}$ can be calculated. ■

Theorem 3.3: *The system $(\hat{A}, \hat{B}, \hat{C})$, given in (12)–(13), is exponentially stabilisable and exponentially detectable on $\mathcal{H}$.*

Proof: First, it is easy to observe that any operator of the form $K = [-\alpha I \quad 0]$, where $\alpha > 0$, exponentially stabilises the pair $(\hat{A}, \hat{B})$. Moreover, it can be shown that $(\hat{A}, \hat{C})$ is exponentially detectable by using Curtain and Zwart (1995, exercise 5.25(h), p.262–263). Indeed, it is easy to prove that $Ker(sI - \hat{A}) \cap Ker(\hat{C}) = \{0\}$. On the other hand, it can be easily shown that $\sigma(\hat{A}) = \sigma(A) \cap \{0\}$ and the associated eigenvectors are given by

$$\boldsymbol{\phi}_0 = \begin{pmatrix} 1 \\ -\mathbf{b} \end{pmatrix} \quad \text{and} \quad \boldsymbol{\phi}_n = \begin{pmatrix} 0 \\ \tilde{\boldsymbol{\phi}}_n \end{pmatrix} \quad n \geq 1, \tag{19}$$

and the eigenvectors of $\hat{A}^*$ are given by

$$\boldsymbol{\psi}_0 = \begin{pmatrix} 1 \\ 0 \end{pmatrix} \quad \text{and} \quad \boldsymbol{\psi}_n = \begin{pmatrix} \frac{1}{\lambda_n}\langle \gamma, \tilde{\boldsymbol{\psi}}_n\rangle_H \\ \tilde{\boldsymbol{\psi}}_n \end{pmatrix} \quad n \geq 1. \tag{20}$$

Moreover, it can be easily shown that the eigenvectors $\{\boldsymbol{\phi}_n, n \geq 0\}$ and $\{\boldsymbol{\psi}_n, n \geq 0\}$ are biorthogonal, i.e. $\langle \boldsymbol{\phi}_n, \boldsymbol{\psi}_m\rangle = \delta_{mn}$. ■

4. Output-feedback boundary control

This section is devoted to crafting an output-feedback controller tailored for the boundary control system described in (5). To accomplish this task, we will introduce a stabilising compensator associated with the augmented system (12).

$$\begin{cases} \dot{\hat{x}}(t) = (\hat{A} + L_o\hat{C})\hat{x}(t) + \hat{B}u(t) - L_o y(t) \\ u(t) = K_o\hat{x}(t), \end{cases} \tag{21}$$

where K_o is the state-feedback operator and L_o is the output injection operator. To find these two operators, the approach involves solving the linear-quadratic control problems linked with both the augmented system (12) and its dual version.

Problem 4.1: Find an optimal input u_o to minimise the cost function

$$J(x_0, u) = \int_0^{\infty} (|y(s)|^2 + r|u(s)|^2)\, \mathrm{d}s \tag{22}$$

along the trajectories of system (12).

Problem 4.2: Find an optimal input $\tilde{u}_o$ to minimise the cost function

$$\tilde{J}(\tilde{x}_0, \tilde{u}) = \int_0^{\infty} (|\tilde{y}(s)|^2 + \tilde{r}|\tilde{u}(s)|^2)\, \mathrm{d}s \tag{23}$$

along the trajectories of the dual system

$$\begin{cases} \dot{\tilde{x}}(t) = \hat{A}^*\tilde{x}(t) + \hat{C}^*\tilde{u}(t) \\ \tilde{y}(t) = \hat{B}^*\tilde{x}(t) \end{cases} \tag{24}$$

Note that the cost functions J and $\tilde{J}$ are the standard quadratic functions in the case of single input and single output with weight functions r and $\tilde{r}$. In Theorem 3.3, it has been shown that the system $(\hat{A}, \hat{B}, \hat{C})$ is exponentially stabilisable and detectable, therefore each of the optimisation problems admits a unique solution that can be found by solving the associated operator Riccati equations (see Bensoussan et al., 2007; Curtain & Zwart, 1995): $\forall\, x, x' \in D(\hat{A})$ and $\forall\, \tilde{x}, \tilde{x}' \in D(\hat{A}^*)$.

$$\langle \hat{A}x, Qx'\rangle + \langle Qx, \hat{A}x'\rangle + \langle \hat{C}x, \hat{C}x'\rangle - \frac{1}{r}\langle \hat{B}^*Qx, \hat{B}^*Qx'\rangle = 0, \tag{25}$$

$$\langle \hat{A}^*\tilde{x}, \Pi\tilde{x}'\rangle + \langle \Pi\tilde{x}, \hat{A}^*\tilde{x}'\rangle + \langle \hat{B}^*\tilde{x}, \hat{B}^*\tilde{x}'\rangle - \frac{1}{\tilde{r}}\langle \hat{C}\Pi\tilde{x}, \hat{C}\Pi\tilde{x}'\rangle = 0 \tag{26}$$

The following theorem shows that the eigenfunctions of the operators $\hat{A}$ and its adjoint can be used to construct the optimal state-feedback operator as well as the output injection operator.

Theorem 4.1: *Let $\hat{A}$ be the operator given by (13) and its adjoint operator $\hat{A}^*$. Let $\{\lambda_n\}_{n\geq 0}$ be the set of eigenvalues of $\hat{A}$ and $\{\boldsymbol{\phi}_n\}_{n\geq 0}$ the corresponding eigenfunctions. Also, let $\{\boldsymbol{\psi}_n\}_{n\geq 0}$ be the eigenfunctions of $\hat{A}^*$. The solutions of the operator Riccati Equations (25) and (26) are given by*

$$Qx = \sum_{n,m=0}^{\infty} Q_{nm}\langle x, \boldsymbol{\psi}_m\rangle \boldsymbol{\psi}_n \quad \text{and}$$

$$\Pi\tilde{x} = \sum_{n,m=0}^{\infty} \Pi_{nm}\langle \tilde{x}, \boldsymbol{\phi}_m\rangle \boldsymbol{\phi}_n, \tag{27}$$

where Q_{nm} and Π_{nm} are solutions of the following sets of algebraic equations:

$$(\lambda_n + \lambda_m)Q_{nm} + \hat{C}_{nm} - \frac{1}{r}\sum_{k,l=0}^{\infty} Q_{nk}Q_{ml}\hat{B}_{kl} = 0, \quad n, m \geq 0 \tag{28}$$

$$(\lambda_n + \lambda_m)\Pi_{nm} + \hat{B}_{nm} - \frac{1}{\tilde{r}}\sum_{k,l=0}^{\infty} \Pi_{nk}\Pi_{ml}\hat{C}_{kl} = 0, \quad n, m \geq 0. \tag{29}$$

Proof: To solve Equation (25), let $x = \boldsymbol{\phi}_n$ and $x' = \boldsymbol{\phi}_m$, then one gets

$$\langle \hat{A}\boldsymbol{\phi}_n, Q\boldsymbol{\psi}_m\rangle + \langle Q\boldsymbol{\phi}_n, \hat{A}\boldsymbol{\phi}_m\rangle + \langle \hat{C}\boldsymbol{\phi}_n, \hat{C}\boldsymbol{\phi}_m\rangle - \frac{1}{r}\langle \hat{B}^*Q\boldsymbol{\phi}_n, \hat{B}^*Q\boldsymbol{\phi}_m\rangle = 0$$

since $\{\boldsymbol{\phi}_n\}_{n\geq 0}$ are the eigenfunctions of $\hat{A}$ with eigenvalues $\{\lambda_n\}_{n\geq 0}$, then

$$\lambda_n\langle \boldsymbol{\phi}_n, Q\boldsymbol{\phi}_m\rangle + \lambda_m\langle Q\boldsymbol{\phi}_n, \boldsymbol{\phi}_m\rangle + \langle \hat{C}\boldsymbol{\phi}_n, \hat{C}\boldsymbol{\phi}_m\rangle - \frac{1}{r}\langle \hat{B}^*Q\boldsymbol{\phi}_n, \hat{B}^*Q\boldsymbol{\phi}_m\rangle = 0.$$

If we put $Q_{nm} = \langle \boldsymbol{\phi}_n, Q\boldsymbol{\phi}_m\rangle$, $\hat{C}_{nm} = \langle \hat{C}\boldsymbol{\phi}_n, \hat{C}\boldsymbol{\phi}_m\rangle$ and $\hat{B}_{nm} = \langle \hat{B}^*\boldsymbol{\psi}_m, \hat{B}^*\boldsymbol{\psi}_n\rangle$, it can be proved that $\langle \hat{B}\hat{B}^*Q\boldsymbol{\phi}_n, Q\boldsymbol{\phi}_m\rangle = \sum_{k,l=0}^{\infty} Q_{nk}Q_{ml}\hat{B}_{kl}$, which means that $Q_{nm} = Q_{mn}$ satisfies the set of algebraic equation (28). On the other hand and to solve Equation (26), the same process is used by taking $\tilde{x} = \boldsymbol{\psi}_n$ and $\tilde{x}' = \boldsymbol{\psi}_m$, then the equation can be written as follows:

$$\lambda_n\langle \boldsymbol{\psi}_n, \Pi\boldsymbol{\psi}_m\rangle + \lambda_m\langle \Pi\boldsymbol{\psi}_n, \boldsymbol{\psi}_m\rangle + \langle \hat{B}^*\boldsymbol{\psi}_n, \hat{B}^*\boldsymbol{\psi}_m\rangle - \frac{1}{\tilde{r}}\langle \hat{C}\Pi\boldsymbol{\psi}_n, \hat{C}\Pi\boldsymbol{\psi}_m\rangle = 0.$$

Consequently, it can be observed that $\Pi_{nm} = \langle \boldsymbol{\psi}_n, \Pi\boldsymbol{\psi}_m\rangle$ satisfies the set of algebraic equation (29). Once the sets of algebraic Equations (28) and (29) are solved then the operators Q and Π can be expressed in terms of the eigenfunctions $\boldsymbol{\phi}_n$ and $\boldsymbol{\psi}_n$, respectively. Indeed, one can use the fact that Qx is an element $\mathcal{H}$ and then it can be expressed in the Riesz basis $\{\boldsymbol{\phi}_n\}_{n\geq 0}$ (see Curtain & Zwart, 1995, lemma 2.3.2)

$$Qx = \sum_{n=0}^{\infty}\langle Qx, \boldsymbol{\phi}_n\rangle\boldsymbol{\psi}_n = \sum_{n=0}^{\infty}\langle x, Q\boldsymbol{\phi}_n\rangle\boldsymbol{\psi}_n = \sum_{n=0}^{\infty}\langle x, \sum_{m=0}^{\infty}\langle Q\boldsymbol{\phi}_n, \boldsymbol{\phi}_m\rangle\boldsymbol{\psi}_m\rangle\boldsymbol{\psi}_n,$$

which yields the expression of the operator Q given in (27). Similar calculations are performed to get the expression of the operator Π given in (27). ■

Now the state-feedback and output injection operators can be expressed as an expansion of the eigenvectors of the operators $\hat{A}$ and $\hat{A}^*$, respectively.

Theorem 4.2: *Let $\hat{A}$ be the operator given in* (13) *and its adjoint operator $\hat{A}^*$. Let $\{\lambda_n\}_{n\geq 0}$ be the set of eigenvalues of $\hat{A}$ and $\{\boldsymbol{\phi}_n\}_{n\geq 0}$ the corresponding eigenfunctions. Also, let $\{\boldsymbol{\psi}_n\}_{n\geq 0}$ be the eigenfunctions of $\hat{A}^*$. The optimal state-feedback and output injection operators are given by*

$$K_o x = -\frac{1}{r}\sum_{m=0}^{\infty}\left[Q_{0m} - \sum_{n=1}^{\infty} Q_{nm}\mathbf{b}_n\right]\langle x, \boldsymbol{\psi}_m\rangle, \quad \forall\, x \in \mathcal{H} \tag{30}$$

$$L_o y = -\frac{1}{\tilde{r}}\sum_{\substack{n=0\\m=1}}^{\infty}\Pi_{nm}\mathbf{c}_m\boldsymbol{\phi}_n y, \quad \forall\, y \in \mathbb{R} \tag{31}$$

where $\mathbf{b}_n = \langle \gamma\lambda_n^{-1} - \mathbf{b}, \tilde{\boldsymbol{\psi}}_n\rangle_H$ and $\mathbf{c}_m = \langle \mathbf{c}, \tilde{\boldsymbol{\phi}}_m\rangle_H$.

Proof: It is known that the state-feedback operator is related to the solution of the operator Riccati equation as follows: $K_o = -\frac{1}{r}\hat{B}^*Q$. Now, let us calculate the state-feedback operator for all $x \in \mathcal{H}$

$$K_o x = -\frac{1}{r}\hat{B}^*Qx = -\frac{1}{r}\sum_{n,m=0}^{\infty}\hat{B}^*Q_{nm}\langle x, \boldsymbol{\psi}_m\rangle\boldsymbol{\psi}_n = -\frac{1}{r}\sum_{m=0}^{\infty}\hat{Q}_{0m}\langle x, \boldsymbol{\psi}_m\rangle\hat{B}^*\boldsymbol{\psi}_0 - \frac{1}{r}\sum_{\substack{n=1\\m=0}}^{\infty}Q_{nm}\langle x, \boldsymbol{\psi}_m\rangle\hat{B}^*\boldsymbol{\psi}_n.$$

By using the expressions of $\boldsymbol{\psi}_0$ and $\boldsymbol{\psi}_n$ given by (20), it can be shown that $\hat{B}^*\boldsymbol{\psi}_0 = 1$ and $\hat{B}^*\boldsymbol{\psi}_n = \langle \gamma\lambda_n^{-1} - \mathbf{b}, \tilde{\boldsymbol{\psi}}_n\rangle_H := \mathbf{b}_n$ and therefore (30) holds.

Now let us calculate the output injection operator but first it should be noted that the output injection operator is the adjoint of the state-feedback operator of the dual system and therefore one gets for all $y \in \mathbb{R}$,

$$\begin{aligned} L_o y &= -\frac{1}{\tilde{r}}\Pi\hat{C}^*y = -\frac{1}{\tilde{r}}\sum_{n,m=0}^{\infty}\Pi_{nm}\langle \hat{C}^*y, \boldsymbol{\phi}_m\rangle\boldsymbol{\phi}_n \\ &= -\frac{1}{\tilde{r}}\sum_{n=0}^{\infty}\Pi_{n0}\langle \hat{C}^*y, \boldsymbol{\phi}_0\rangle\boldsymbol{\phi}_n - \frac{1}{\tilde{r}}\sum_{\substack{n=0\\m=1}}^{\infty}\Pi_{nm}\langle \hat{C}^*y, \boldsymbol{\phi}_m\rangle\boldsymbol{\phi}_n \\ &= -\frac{1}{\tilde{r}}\sum_{n=0}^{\infty}\Pi_{n0}\langle \hat{C}^*y, \boldsymbol{\phi}_0\rangle\boldsymbol{\phi}_n \\ &\quad - \frac{1}{\tilde{r}}\sum_{\substack{n=0\\m=1}}^{\infty}\Pi_{nm}\left\langle \begin{pmatrix} \langle \mathbf{b}, \mathbf{c}y\rangle \\ \mathbf{c}y \end{pmatrix}, \begin{pmatrix} 0 \\ \tilde{\boldsymbol{\phi}}_m \end{pmatrix}\right\rangle\boldsymbol{\phi}_n. \end{aligned}$$

Due to simple calculations, it can be observed that $\hat{C}\boldsymbol{\phi}_0 = 0$, which means that the first term equals to zero and since y is constant, then one gets the expression of the output injection operator (30). ■

Now, based on the state-feedback and output injection operators, it is possible to construct the stabilising compensator for the boundary control system.

Theorem 4.3: *Let us consider the boundary control system given in (5)–(8). Let $\{\lambda_n\}_{n\geq 1}$ be the set of eigenvalues of A and $\{\tilde{\boldsymbol{\phi}}_n\}_{n\geq 1}$ the corresponding eigenvectors. Also, let $\{\tilde{\boldsymbol{\psi}}_n\}_{n\geq 1}$ be the eigenvectors of A^*. The stabilising compensator is given by*

$$\hat{z}(t) = \sum_{n=1}^{\infty} \langle \hat{z}(t), \tilde{\boldsymbol{\psi}}_n \rangle_H \tilde{\boldsymbol{\phi}}_n := \sum_{n=1}^{\infty} \hat{z}_n(t) \tilde{\boldsymbol{\phi}}_n, \tag{32}$$

where $\{\hat{z}_n\}_{n\geq 1}$ are the solutions of the following linear differential equations:

$$\begin{aligned} \dot{\hat{z}}_n(t) &= \lambda_n \hat{z}_n(t) + \lambda_n \mathbf{b}_n w(t) \\ &\quad + \frac{1}{\tilde{r}} \sum_{m=1}^{\infty} \Pi_{nm} \mathbf{c}_m \left[y(t) - \sum_{k=1}^{\infty} \mathbf{c}_k \hat{z}_k(t) \right] \end{aligned} \tag{33}$$

with the optimal feedback boundary control on the estimated state is given by

$$w(t) = \mathrm{e}^{At} \left[\int_0^t A_m \, \mathrm{e}^{-A\tau} \hat{z}_m(\tau) \, \mathrm{d}\tau \right] \tag{34}$$

where $A_m = \frac{1}{r} \sum_{n=1}^{\infty} (Q_{nm} \mathbf{b}_n - Q_{0m})$ and $A = \sum_{m=0}^{\infty} A_m \mathbf{b}_m$.

Proof: To construct the stabilising compensator, the general form (21) will be employed. The eigenvector expansions of the state-feedback operator output injection operators as well as the expansion of the operator $\hat{A}$ will be implemented to design the compensator. In this case, the compensator (21) becomes

$$\begin{aligned} \sum_{n=0}^{\infty} \langle \dot{\hat{x}}(t), \boldsymbol{\psi}_n \rangle \boldsymbol{\phi}_n &= \sum_{n=0}^{\infty} \lambda_n \langle \hat{x}(t), \boldsymbol{\psi}_n \rangle \boldsymbol{\phi}_n + \sum_{n=0}^{\infty} \langle \hat{B} u(t), \boldsymbol{\psi}_n \rangle \boldsymbol{\phi}_n \\ &\quad - \frac{1}{\tilde{r}} \sum_{\substack{n=0\\m=1}}^{\infty} \Pi_{nm} \mathbf{c}_m \boldsymbol{\phi}_n \left[\hat{C} \hat{x}(t) - y(t) \right]. \end{aligned} \tag{35}$$

Indeed, the idea is to express the elements of Equation (21) in terms of the Riesz basis $\{\boldsymbol{\phi}_n\}_{n\geq 0}$ and its bio-orthogonal basis $\{\boldsymbol{\psi}_n\}_{n\geq 0}$ (see Curtain & Zwart, 1995, Lemma 2.3.2). The last term of Equation (35) is a consequence of the expression of L_o given by Equation (31). By matching term by term, Equation (35) will lead to the following set of differential equations for $n \geq 0$.

$$\begin{aligned} \langle \dot{\hat{x}}(t), \boldsymbol{\psi}_n \rangle &= \lambda_n \langle \hat{x}(t), \boldsymbol{\psi}_n \rangle + \langle \hat{B} u(t), \boldsymbol{\psi}_n \rangle \\ &\quad - \frac{1}{\tilde{r}} \sum_{m=1}^{\infty} \Pi_{nm} \mathbf{c}_m \left[\hat{C} \hat{x}(t) - y(t) \right]. \end{aligned} \tag{36}$$

By using Equation (11) for the estimated state and by performing straightforward calculations, it is easy to prove the following identities:

$$\langle \dot{\hat{x}}(t), \boldsymbol{\psi}_0 \rangle = \dot{\hat{w}}(t), \quad \langle \hat{B} u(t), \boldsymbol{\psi}_0 \rangle = u(t)$$

$$\begin{aligned} \langle \dot{\hat{x}}(t), \boldsymbol{\psi}_n \rangle &= \langle \dot{\hat{z}}(t), \tilde{\boldsymbol{\psi}}_n \rangle_H + \frac{\dot{w}}{\lambda_n} \langle \gamma, \tilde{\boldsymbol{\psi}}_n \rangle_H \\ &\quad - \langle B \dot{w}, \tilde{\boldsymbol{\psi}}_n \rangle_H, \quad n \geq 1 \\ \langle \hat{x}(t), \boldsymbol{\psi}_n \rangle &= \langle \hat{z}(t), \tilde{\boldsymbol{\psi}}_n \rangle_H + \frac{w}{\lambda_n} \langle \gamma, \tilde{\boldsymbol{\psi}}_n \rangle_H \\ &\quad - \langle B w, \tilde{\boldsymbol{\psi}}_n \rangle_H, \quad n \geq 1 \\ \langle \hat{B} u(t), \boldsymbol{\psi}_n \rangle &= \frac{\dot{w}}{\lambda_n} \langle \gamma, \tilde{\boldsymbol{\psi}}_n \rangle_H - \langle B \dot{w}, \tilde{\boldsymbol{\psi}}_n \rangle_H \\ &= \langle \mathbf{b}_n, \tilde{\boldsymbol{\psi}}_n \rangle_H \dot{w}(t), \quad n \geq 1 \\ \hat{C} \hat{x}(t) &= \mathcal{C} \hat{z}(t) = \langle \mathbf{c}, \hat{z}(t) \rangle_H = \sum_{k=1}^{\infty} \mathbf{c}_k \hat{z}_k(t). \end{aligned}$$

Therefore, Equation (36) can be written for $n = 0$ as follows (remember that $\lambda_0 = 0$):

$$\dot{\hat{w}}(t) = u(t) - -\frac{1}{\tilde{r}} \sum_{m=1}^{\infty} \Pi_{0m} \mathbf{c}_m \left[\hat{C} \hat{x}(t) - y(t) \right].$$

However, since w is the input function and it is not required to be estimated, then $\hat{w}(t) = w(t)$, which means that one can choose $\Pi_{0m} = 0, \forall\, m \geq 1$ and in this case the output injection operator becomes

$$L_o y = -\frac{1}{\tilde{r}} \sum_{\substack{n=1\\m=1}}^{\infty} \Pi_{nm} \mathbf{c}_m \boldsymbol{\phi}_n y, \quad \forall\, y \in \mathbb{R}.$$

For the case when $n \geq 1$, Equation (36) leads to the following set of differential equations:

$$\begin{aligned} &\langle \dot{\hat{z}}(t), \boldsymbol{\psi}_n \rangle_H \\ &= \lambda_n \langle \hat{z}(t), \boldsymbol{\psi}_n \rangle_H + \lambda_n \langle \lambda_n^{-1} \gamma, \tilde{\boldsymbol{\psi}}_n \rangle_H w(t) - \lambda_n \langle \mathbf{b}, \tilde{\boldsymbol{\psi}}_n \rangle_H w(t) \\ &\quad - \frac{1}{\tilde{r}} \sum_{m=1}^{\infty} \Pi_{nm} \mathbf{c}_m \left[\sum_{k=1}^{\infty} \mathbf{c}_k \hat{z}_k(t) - y(t) \right], \end{aligned}$$

which means that the components of the compensator $\hat{z}_n(t) := \langle \hat{z}(t), \tilde{\boldsymbol{\psi}}_n \rangle_H$ satisfy the set of differential equation (33). ∎

On the other hand, by using the state-feedback operator expression (30), one gets the expression of the input u in terms of the estimated state.

$$u(t) = -\frac{1}{r} \sum_{m=0}^{\infty} \left[Q_{0m} - \sum_{n=1}^{\infty} Q_{nm} \mathbf{b}_n \right] \langle \hat{x}, \boldsymbol{\psi}_m \rangle.$$

It is known that $u(t) = \dot{w}(t)$ and also $\hat{w}(t) = w(t)$. Hence, one gets the following linear differential equation:

$$\dot{w}(t) = -\frac{1}{r} \sum_{m=0}^{\infty} \left[Q_{0m} - \sum_{n=1}^{\infty} Q_{nm} \mathbf{b}_n \right] \left[\hat{z}_m(t) + \mathbf{b}_m w(t) \right],$$

which can be written under the following standard form of a linear differential equation:

$$\dot{w}(t) + \frac{1}{r} \sum_{m=0}^{\infty} \mathbf{b}_m \left[Q_{0m} - \sum_{n=1}^{\infty} Q_{nm} \mathbf{b}_n \right] w(t)$$

$$= \frac{1}{r} \sum_{m=0}^{\infty} \left[\sum_{n=1}^{\infty} Q_{nm} \mathbf{b}_n - Q_{0m} \right] \hat{z}_m(t).$$

If we put $A_m = \frac{1}{r} \sum_{n=1}^{\infty} (Q_{nm}\mathbf{b}_n - Q_{0m})$ and $A = \sum_{m=0}^{\infty} A_m b_m$, then the equation becomes

$$\dot{w}(t) - Aw(t) = \sum_{m=0}^{\infty} A_m \hat{z}_m(t), \quad w(0) = 0,$$

whose solution is given by (34). Note that the initial condition $w(0) = 0$ is a consequence of Equation (4).

Remark 4.1: Note that the output feedback controller is developed based on the linearised version of the PDE model, which means that all the results are valid locally around the chosen steady-state profile. To study the performance of the designed regulator for the non-linear system both closed-loop stability and optimality should be investigated. For the closed-loop stability, some tools similar to the ones in Aksikas et al. (2008, section 5.1) should be developed. On the other hand, the optimality analysis is based on the famous inverse optimal control problem, which mainly focuses on the question: what type of modification of the cost criteria (22) and (23) can restore optimality. This problem has been already investigated by the author in Aksikas et al. (2008, section 5.2) in which it is shown that under the asymptotic stability of the closed-loop system, then the state-feedback controller (30) and the output injection estimator (31) are optimal with respect to the following modified cost criteria:

$$\mathcal{J}(x_0, u) = \int_0^\infty (|y(s)|^2 - 2\langle h, Qx\rangle + r|u(s)|^2)\, ds$$

$$\tilde{\mathcal{J}}(\tilde{x}_0, \tilde{u}) = \int_0^\infty (|\tilde{y}(s)|^2 - 2\langle \tilde{h}, \Pi\tilde{x}\rangle + \tilde{r}|\tilde{u}(s)|^2)\, ds,$$

where h and $\tilde{h}$ are somehow related to the nonlinear part of the system.

5. Numerical simulations

This section is devoted to the numerical simulations to show the performance of the designed output feedback regulator. First, it is important to note that the computational demands associated with implementing the algorithm can be influenced by the infinite series representation of both the feedback controller and the output injection operator. To facilitate simulations, a finite selection of modes must be made, potentially impacting the algorithm's efficacy. To ensure that the algorithm's performance remains above certain predefined error thresholds, a comprehensive analysis can be conducted to determine the optimal number of modes required. It is also an important issue for practical implementation. The values of the model parameters are given in Table 1.

The main control objective is to drive the trajectory of Y_B to a target profile. Then by using the operating conditions, the steady-state equations (3) are solved to get the equilibrium profiles associated with the desired profile of Y_B, which are shown in Figure 1. On the other hand, the algebraic equation (16) is solved numerically to get the sequence ω_n and then the spectrum of the operators $\mathcal{A}_{11}$ and $\mathcal{A}_{22}$ are calculated by using Equations (15) and (18). The first five eigenvalues of each operator are given in

Table 1. Model parameters.

Parameter	Value	Unit
D_a	0.5	$m^2 \times hr^{-1}$
v	2	$m \times hr^{-1}$
k_0	22.9	$(h \times \text{weight fraction})^{-1}$
k_1	18.1	$(h \times \text{weight fraction})^{-1}$
k_2	1.7	$(h \times \text{weight fraction})^{-1}$
$Y_{1,in}$	0.7	weight fraction
$Y_{2,in}$	0	weight fraction

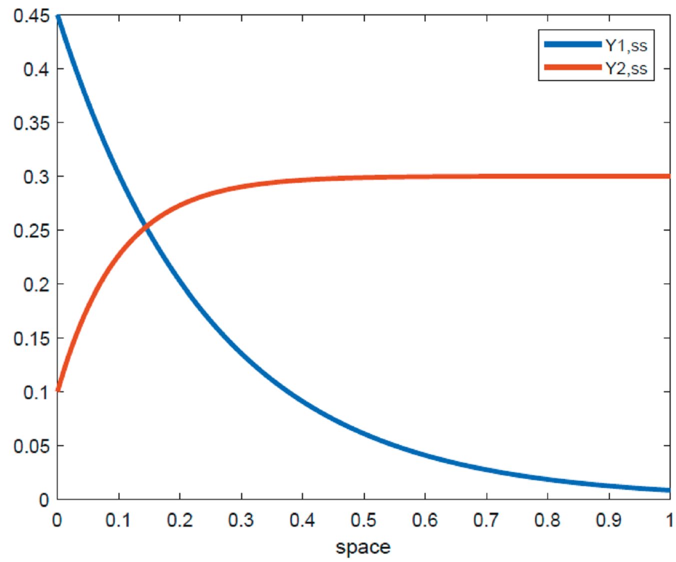

Figure 1. Steady-state profiles $\overline{Y}_1$ and $\overline{Y}_2$.

Table 2. The first five eigenvalues.

n	ω_n	μ_n	η_n
1	4.058	−20.68	−10.93
2	6.851	−35.92	−26.17
3	9.826	−60.73	−50.98
4	12.875	−95.33	−85.58
5	15.957	−139.75	−130

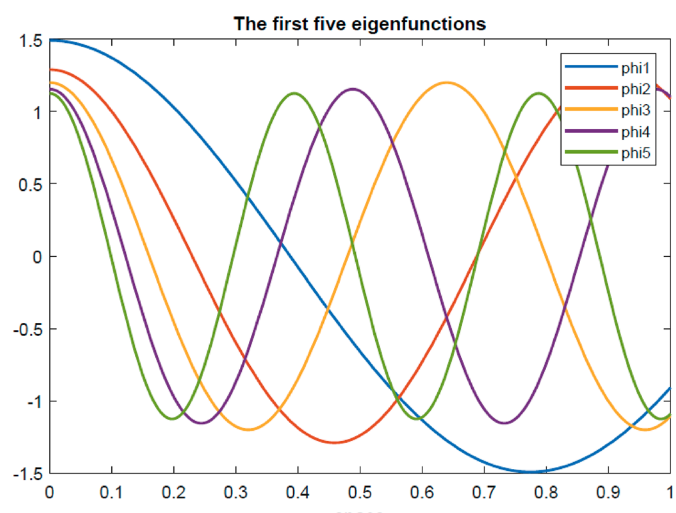

Figure 2. The first five eigenfunctions for $\mathcal{A}_{11}$ and $\mathcal{A}_{22}$.

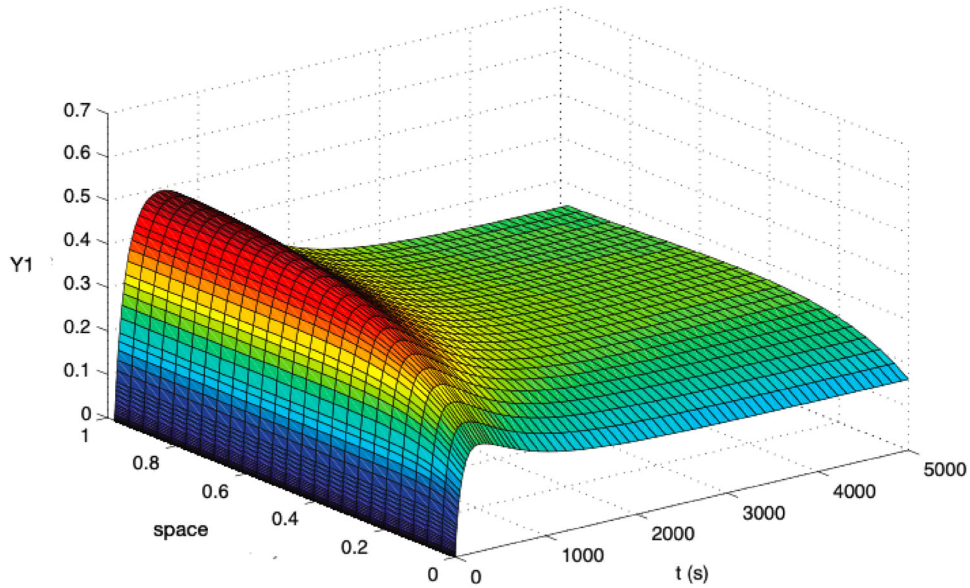

Figure 3. Closed-loop trajectory of Y_2 under the output-feedback regulator.

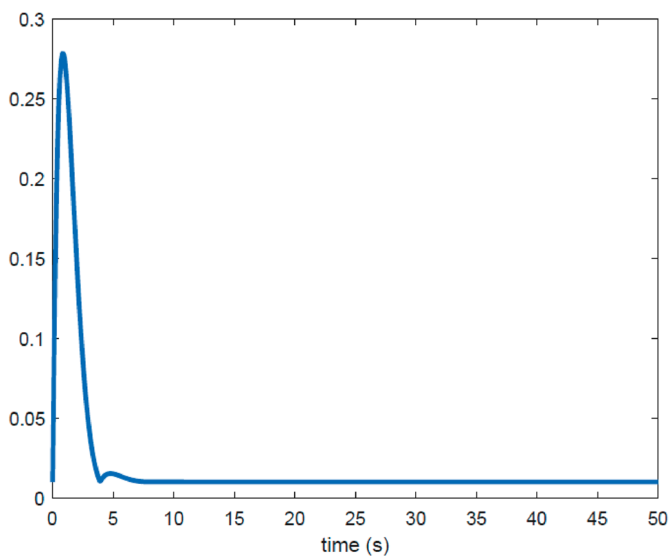

Figure 4. Norm of the error between the state Y_1 and the estimated state.

Table 2, which are all combined giving the first 10 eigenvalues of $\mathcal{A}$ (Figure 2).

Numerical simulations are performed to test the performance of the developed output-feedback regulator. The two sets of algebraic equations (28)) and (29) are solved to compute Q_{nm} and Π_{nm}. The fact that Q and P are self-adjoint operators helps reduce the calculations since in this case $Q_{nm} = Q_{mn}$ and $\Pi_{nm} = \Pi_{mn}$. The closed-loop boundary control system (5) is simulated by using the feedback control (34) applied to the estimated state which is calculated by solving the set of differential equation (21). Numerical simulations were performed by using finite difference discretisation-based method and the Matlab function ode15s. Figure 3 shows the closed-loop trajectory of gasoline under the designed output feedback regulator. It can be observed that the regulator drive the process to its steady state. Moreover, as it is expected the compensator gives a good estimate of the process states. Indeed, Figure 4 shows the norm of the error between the system state and the estimated state. It can be seen that the error converges exponentially to zero.

6. Conclusion and future work

An output feedback boundary control of a catalytic cracking reactor has been developed based on a parabolic PDE model. Infinite-dimensional linearised version of the model has been employed to find both the state-feedback operator and output injection operator. Both are formulated in terms of the eigenvalues and eigenvectors of the system generator. Numerical simulations have been performed to show the performance of the optimal output-feedback regulator. The work developed here is to be extended to a more general case of boundary control parabolic PDE system. This is under investigation by the author.

Acknowledgements

This work is supported by Qatar University Grant CDIRCC- 2023-112. The authors confirm that there are no relevant financial or non-financial competing interests to report.

Disclosure statement

No potential conflict of interest was reported by the author(s).

Data availability statement

The author confirms that the data supporting the findings of this study are available within the article and its supplementary materials.

References

Ahmed-Ali, T., Giri, F., Krstic, M., & Lamnabhi-Lagarrigue, F. (2015). Observer design for a class of nonlinear ODE–PDE cascade systems. *Systems & Control Letters*, *83*, 19–27. https://doi.org/10.1016/j.sysconle.2015.06.003

Aksikas, I. (2020). Duality-based optimal compensator for boundary control hyperbolic PDEs system : Application to a tubular cracking reactor. *Journal of the Franklin Institute*, *357*(14), 9692–9708. https://doi.org/10.1016/j.jfranklin.2020.07.033

Aksikas, I. (2021a). Optimal control and duality-based observer design for a hyperbolic PDEs system with application to fixed-bed reactor. *International Journal of Systems Science*, *52*(12), 2493–2504. https://doi.org/10.1080/00207721.2021.1890856

Aksikas, I. (2021b). Optimal output-feedback temperature regulation of a catalytic reverse flow reactor PDEs model. *Journal of Process Control*, *103*, 1–7. https://doi.org/10.1016/j.jprocont.2021.05.004

Aksikas, I., Mohammadi, L., Forbes, J. F., Belhamadia, Y., & Dubljevic, S. (2013). Optimal control of an advection-dominated catalytic fixed-bed reactor with catalyst deactivation. *Journal of Process Control*, *23*(10), 1508–1514. https://doi.org/10.1016/j.jprocont.2013.09.016

Aksikas, I., Winkin, J. J., & Dochain, D. (2004). Stability analysis of an infinite-dimensional linearised plug flow reactor model. In *The 43rd IEEE Conference on Decision and Control*, (Vol. 4, pp. 2417–2422). IEEE.

Aksikas, I., Winkin, J., & Dochain, D. (2008). Optimal LQ-feedback control for a class of first-order hyperbolic distributed parameter systems. *ESAIM: Control, Optimisation and Calculus of Variations*, *14*(4), 897–908.

Bensoussan, A., Da Prato, G., Delfour, M. C., & Mitter, S. K. (2007). *Representation and control of infinite dimensional systems* (2nd ed.). Birkhauser.

Bošković, D. M., Balogh, A., & Krstić, M. (2003). Backstepping in infinite dimension for a class of parabolic distributed parameter systems math. *Control Signals Systems*, *16*(1), 44–75. https://doi.org/10.1007/s00498-003-0128-6

Bošković, D. M., & Krstić, M. (2002). Backstepping control of chemical tubular reactors. *Computers & Chemical Engineering*, *26*(7-8), 1077–1085. https://doi.org/10.1016/S0098-1354(02)00026-1

Bounit, H., & Hammouri, H. (1997). Observers for infinite-dimensional bilinear systems. *European Journal of Control*, *3*(4), 325–339. https://doi.org/10.1016/S0947-3580(97)70090-6

Christofides, P. D. (1998). Robust control of parabolic PDE systems. *Chemical Engineering Science*, *53*(16), 2949–2965. https://doi.org/10.1016/S0009-2509(98)00091-8

Christofides, P. D. (2001). *Nonlinear and robust control of partial differential equation systems: Methods and application to transport-reaction processes*. Birkhauser.

Christofides, P. D., & Daoutidis, P. (1996). Feedback control of hyperbolic PDE systems. *AICHE Journal*, *42*(11), 3063–3086. https://doi.org/10.1002/aic.v42:11

Curtain, R. F., & Zwart, H. J. (1995). *An introduction to infinite-dimensional linear systems theory*. Springer-Verlag.

De Monte, F. (2002). An analytic approach to the unsteady heat conduction processes in one-dimensional composite media. *International Journal of Heat and Mass Transfer*, *45*(6), 1333–1343. https://doi.org/10.1016/S0017-9310(01)00226-5

Deutscher, J. (2013). Finite-dimensional dual state feedback control of linear boundary control system. *International Journal of Control*, *86*(1), 41–53. https://doi.org/10.1080/00207179.2012.717723

Dochain, D. (2016). Analysis of the multiplicity of equilibrium profiles in tubular reactor models. *IFAC-PaperOnLine*, *49*(18), 903–908. https://doi.org/10.1016/j.ifacol.2016.10.281

Dubljevic, S., & Christofides, P. D. (2006). Predictive control of parabolic PDEs with boundary control actuation. *Chemical Engineering Science*, *61* (18),6239–6248. https://doi.org/10.1016/j.ces.2006.05.041

Dubljevic, S., El-Farra, N. E., Mhaskar, P., & Christofides, P. D. (2006). Predictive control of parabolic PDEs with state and control constraints. *International Journal of Robust and Nonlinear Control*, *16* (16),749–772. https://doi.org/10.1002/rnc.v16:16

Gary, J. H., & Handwerk, G. E. (2001). *Petroleum refining: Technology and economics* (4th ed.). CRC Press.

Hanczyz, E. M., & Palazoglu, A. (1995). Sliding mode control of nonlinear distributed parameter chemical processes. *Industrial & Engineering Chemistry Research*, *34* (2), 557–566. https://doi.org/10.1021/ie00041a016

Khatibi, S., Cassol, G. O., & Dubljevic, S. (2021). Model predictive control of a non-isothermal axial dispersion tubular reactor with recycle. *Computers & Chemical Engineering*, *145*, 107159. https://doi.org/10.1016/j.compchemeng.2020.107159

Li, M., & Christofides, P. D. (2008). Optimal control of diffusion–convection–reaction processes using reduced-order models. *Computer And Chemical Engineering*, *32*(9), 2123–2135. https://doi.org/10.1016/j.compchemeng.2007.10.018

Liu, Y., Chen, X., Mei, Y., & Wu, Y. (2022). Observer-based boundary control for an asymmetric output-constrained flexible robotic manipulator. *Science China Information Sciences*, *65*(3), 139203. https://doi.org/10.1007/s11432-019-2893-y

Liu, Y., Guo, F., He, X., & Hui, Q. (2019). Boundary control for an axially moving system with input restrictions based on disturbance observers. *IEEE Transactions on Systems Man and Cybernetics: Systems*, *49*(11), 2242–2253. https://doi.org/10.1109/TSMC.6221021

Moghadam, A. A., Aksikas, I., Dubljevic, S., & Forbes, J. F. (2012). Infinite-dimensional LQ control of a dimethyl ether (DME) catalytic distillation column. *Journal of Process Control*, *22*(9), 1655–1669. https://doi.org/10.1016/j.jprocont.2012.06.018

Mohammadi, L., Aksikas, I., Dubljevic, S., & Forbes, J. F. (2012). LQ-boundary control of a diffusion-convection-reaction system. *International Journal of Control*, *85*(2), 171–181. https://doi.org/10.1080/00207179.2011.642308

Pakravesh, H., Aksikas, I., Votsmeier, M., Dubljevic, S., Hayes, R. E., & Forbes, J. F. (2016). Characteristics-based model predictive control of selective catalytic reduction in diesel-powered vehicles. *Journal of Process Control*, *47*, 98–110. https://doi.org/10.1016/j.jprocont.2016.09.008

Ray, W. H. (1981). *Advanced process control*. McGraw Hill.

Reyes, H. A. F., Schaum, A., Meurer, T., & Alvarez, J. (2020). Stabilization of an unstable tubular reactor by nonlinear passive output feedback control. *Journal of Process Control*, *93*, 83–96. https://doi.org/10.1016/j.jprocont.2020.07.005

Shang, H., Forbes, J. F., & Guay, M. (2000). Feedback control of hyperbolic PDE systems. In: *Advanced control of chemical processes*. IFAC.

Sira-Ramirez, H. (1989). Distributed sliding mode control is systems described by quasilinear partial differential equations. *Systems and Control Letters*, *13*(2), 177–181. https://doi.org/10.1016/0167-6911(89)90036-4

Smyshlyaev, A., & Krstic, M. (2005). Backstepping observers for a class of parabolic PDEs. *Systems & Control Letters*, *54*(7), 613–625. https://doi.org/10.1016/j.sysconle.2004.11.001

Varma, A., & Amundson, N. R. (1973). Some observations on uniqueness and multiplicity of steady states in non-adiabatic chemically reacting systems. *The Canadian Journal of Chemical Engineering*, *51*(2), 206–226. https://doi.org/10.1002/cjce.v51:2

Vries, D., Keesman, K. J., & Zwart, H. (2007). A Luenberger observer for infinite-dimensional bilinear system: A UV disinfection example. In *Symposium on system, structure and control* IFAC.

Weekman V. W., Jr. (1969). Kinetics and dynamics of catalytic cracking selectivity in fixed bed reactors. *Industrial and Engineering Chemistry Process Design and Development*, *8*(3), 385–391. https://doi.org/10.1021/i260031a015

Xu, C. Z., Ligaius, P., & Gauthier, J. P. (1995). An observer for infinite-dimensional dissipative bilinear systems. *Computers & Mathematics with Applications*, *29*(7), 13–21. https://doi.org/10.1016/0898-1221(95)00014-P

Zhou, W., Hamroun, B., Le Gorrec, Y., & Couenne, F. (2015). Lyapunov based nonlinear control of tubular chemical reactors. *IFAC-PapersOnLine*, *48*(8), 1045–1050. https://doi.org/10.1016/j.ifacol.2015.09.106